

# Design and Implementation of Robust Symmetric Attitude Controller for ETS-VIII Spacecraft

T. Nagashio\* T. Kida\* T. Ohtani\*\* Y. Hamada\*\*

\* *University of Electro-Communications, Tokyo, Japan*

(*e-mail: nagasio@mce.uec.ac.jp, kida@mce.uec.ac.jp*)

\*\* *Japan Aerospace Exploration Agency, Tokyo, Japan*

---

**Abstract:** This paper studies the robust attitude control of the large flexible communication satellite ETS-VIII. As a controller candidate, we propose a two-degrees-of-freedom control based on robust direct velocity and displacement feedback, in order to develop a baseline of future controller design technology for this class of spacecraft. For this purpose, the spacecraft modeling and controller synthesis methods are discussed. Then, the controller implementation for on-orbit control experiment is shown with some simulation results.

---

## 1. INTRODUCTION

According to the increasing mission requirement, there is a trend that recent communication satellites have large flexible communication antenna reflectors and solar paddles. During the past three decades, the issues of modeling and control technologies of large spacecraft have been studied extensively, and some on-orbit control experiment results have been reported. As one of them, we have performed the on-orbit attitude control experiment using Engineering Test Satellite VI (ETS-VI) in 1994 (Kida et al. [1997]). Based on the experience, we are now planning an on-orbit experiment of robust control of Engineering Test Satellite VIII (ETS-VIII) launched into Geo-synchronous orbit in December, 2006. It is the largest satellite that Japan has ever developed with measurements that are  $40 \times 37$  (m) and weight 3000 (kg) (Fig. 1). The main mission is mobile communications for which two large deployable reflectors (LDR) are appended in the roll axis direction. A pair of solar paddles (PDL) rotate around the pitch axis at the rate of 360 (deg/day) to direct its normal direction to the Sun. Spacecraft dynamics around three axes are coupled with each other and system parameters drastically change according to paddle rotation. Therefore, it must be treated as a linear parameter varying (LPV) multi-input multi-output (MIMO) system. For this spacecraft, we have studied to apply  $\mu$  synthesis and  $H_\infty$  gain-scheduling controller (Nagashio and Kida [1999], Hamada et al. [2006]). While the controllers obtained using such parametric approaches achieve high control performance, they become higher-order and sensitive to plant parameter accuracy. As another approach, the use of the symmetric static output feedback control is known to be effective for flexible spacecraft with collocated sensors and actuators (Joshi [1986]). It guarantees the robust stability of the closed-loop system irrespective of the system parameters. This paper proposes to construct two-degrees-of freedom controller based on symmetric controller having the salient stability property in order to meet the ETS-VIII spacecraft mission. The optimization methods of feedback controller gains and feedforward controllers are discussed. Finally, on-board

computer implementation problems are discussed, the on-orbit experiment plan and some simulation results are shown.

## 2. SPACECRAFT MODEL

The dynamical equation of ETS-VIII is given by the following hybrid equation (Likins [1970]) when PDL rotation is sufficiently slow.

$$J(\delta)\ddot{\theta} + \sum_i \Delta_i(\delta)\ddot{\eta}_i = u + w \quad (1)$$

$$\Delta_i^T(\delta) + \ddot{\eta}_i + 2\zeta_i\Omega_i\dot{\eta}_i + \Omega_i^2\eta_i = 0 \quad (2)$$

where  $i = n, s, a, b$  denotes the north/south solar paddles and a/b antenna reflectors, and  $\delta \in \mathbb{R}$  is paddle rotation angle.  $\theta \in \mathbb{R}^3$  is attitude angle,  $u \in \mathbb{R}^3$ ,  $w \in \mathbb{R}^3$  are torque control input and disturbance input around three axes and  $\eta_i \in \mathbb{R}^{n_i}$  is modal coordinate of the  $i$  th appendage.  $\Omega_i^2 = \text{diag}[\omega_{i1}^2, \dots, \omega_{in_i}^2]$  is modal stiffness matrix where  $\omega_{ij} \in \mathbb{R}$  and  $\zeta_i \in \mathbb{R}$  denote modal frequency and damping ratio. The inertia matrix  $J(\delta)$  and coupling matrix  $\Delta_i(\delta)$  vary depending on paddle angle  $\delta$ . On the measurement output, by the attitude determination logic based on gyros and earth/sun sensors, the estimated attitude angles and their rates are available.

$$y_1 = \theta, \quad y_2 = \dot{\theta}. \quad (3)$$

From FEM analysis of each appendage under the cantilever condition, coupling matrices and modal parameters of eight modes for LDR ( $n_a = n_b = 8$ ) and eight modes for PDL ( $n_n = n_s = 8$ ) are obtained. The cantilever modal frequency  $\omega_{ij}$  ranges from 0.06 (Hz) to 4.0 (Hz). Thus the obtained full-order model has  $n = 3$  (rigid mode) +  $n_a + n_b + n_n + n_s = 35$  coordinates. The dependency of the spacecraft model on paddle angle  $\delta$  is evaluated by singular value plots of open-loop plant from control input  $u$  to measurement output  $y_1$  for paddle angle  $\delta = 0, 45, 90$  (deg) (Fig. 2). It is apparent that many vibration modes exist in the lower frequency range and they are exchanged with each other according to the paddle rotation.

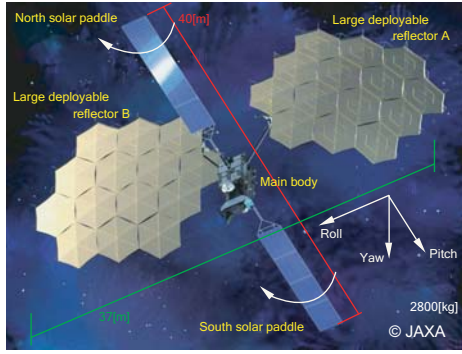


Fig. 1. A view of ETS-VIII.

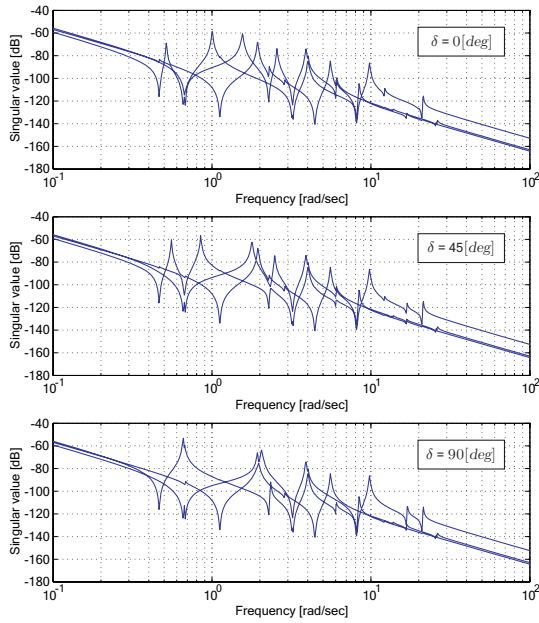


Fig. 2. Singular value plots of ETS-VIII open-loop system for  $\delta = 0, 45$  and  $90$  (deg) from top to bottom.

The controller design objective is to obtain a reduced order controller that robustly stabilizes the LPV MIMO spacecraft against the unstructured uncertainties of higher vibration modes and the structured uncertainties caused by the inaccuracy of modal identification before launch. As well as the closed-loop asymptotic stability, other control specifications must be considered from its mission requirement. They are

- Robust stability for all paddle angles,
- Steady state attitude error less than  $0.05$ (deg) under orbit control thruster firing,
- Attitude tracking capability to  $\pm 0.05$  (deg) step command.

After trade-off studies, we have determined to employ two-degrees-of-freedom control based on the static output feedback controller as stated in the next section. For the controller design, the spacecraft equations (1)(2) and (3) are compactly described as follows.

$$M(\delta)\ddot{p} + D\dot{p} + Kp = Lu + Lw \quad (4)$$

$$y_1 = L^T p, \quad y_2 = L^T \dot{p} \quad (5)$$

where  $p = [\theta^T \eta_a^T \eta_b^T \eta_n^T \eta_s^T]^T \in \mathbb{R}^n$ . It is noted that (4)(5) satisfies two features. First,

$$M(\delta) > 0, \quad D \geq 0, \quad K \geq 0, \quad \forall \delta \in \mathbb{R} \quad (6)$$

hold from the modal identity (Likins [1970]). Second, system (4)(5) is stabilizable and detectable, since the rank conditions

$$\text{rank}[K, L] = \text{rank}[D, L] = n. \quad (7)$$

are satisfied for all  $\delta$  (Ikeda et al. [1993]).

### 3. CONTROLLER DESIGN

The block diagram of the proposed controller is shown in Fig. 3. It consists of the feedback control part of  $K_0$ , and the feedforward part of stable transfer functions  $K_1$  and  $K_2$ . The input-output relation from the reference signal  $r$  and disturbance  $w$  to the measurement output  $y = [y_1^T \ y_2^T]^T$  is given by

$$y = G_{yr}r + G_{yw}w \quad (8)$$

where

$$G_{yw} = (I + PK_0)^{-1}P, \quad G_{yr} = G_{yw}(K_2 + K_0K_1) \quad (9)$$

if we denote the plant transfer function by  $P$ . We first design  $K_0$  so that the closed-loop system is robustly stable and has disturbance attenuation capability to  $w$ . Afterward,  $K_1$  and  $K_2$  are designed so that the output  $y$  quickly follows the step command  $r$  without steady-state error.

#### 3.1 Feedback Control

**Robust stability** Let us consider a static output feedback controller.

$$u = -K_0y \quad (10)$$

where  $K_0 = [K_{01} \ K_{02}]$  and gain matrices  $K_{01}$  and  $K_{02}$  are constant and satisfy

$$K_{01} > 0, \quad K_{02} > 0 \quad (11)$$

Then the closed-loop system (4)(5) with (10) is

$$M(\delta)\ddot{p} + D^*\dot{p} + K^*p = Lw \quad (12)$$

where

$$K^* = K + LK_{01}L^T, \quad D^* = D + LK_{02}L^T. \quad (13)$$

In order to examine the stability of (12), we use the following two lemmas.

Lemma 1 (Ikeda et al. [1993]): The coefficient matrices of (12) satisfy

$$D^* > 0, \quad K^* > 0 \quad (14)$$

if system (4)(5) is stabilizable and detectable.  $\square$

Lemma 2: If  $X, Y > 0$ , there exist a sufficiently small scalar  $\alpha > 0$  such that

$$\begin{bmatrix} X & \alpha Y \\ \alpha Y & Y \end{bmatrix} > 0, \quad \begin{bmatrix} \alpha X & \alpha Y \\ \alpha Y & Y \end{bmatrix} > 0 \quad (15)$$

Proof: It is apparent from Schur complement.  $\square$

Then we can state the following stability condition.

Theorem 1: System (12) is asymptotically stable for all  $\delta \in \mathbb{R}$  if  $M(\delta) > 0$  and  $K^*, D^* > 0$  when disturbance input  $w = 0$ .

Proof: The asymptotic stability of (12) is equivalent to

$$A = \begin{bmatrix} 0 & I \\ -M^{-1}(\delta)K^* & -M^{-1}(\delta)D^* \end{bmatrix} \quad (16)$$

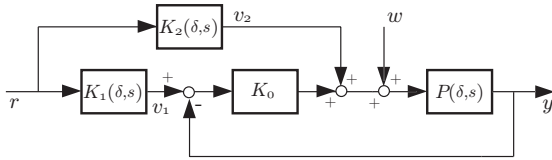


Fig. 3. Block diagram of two-degrees-of-freedom controller.

being stable. The matrix  $A$  is stable if and only if there exists a matrix  $X > 0$  such that

$$XA + A^T X < 0 \quad (17)$$

The Lyapunov inequality obviously has a solution

$$X_e = \begin{bmatrix} K^* & \alpha M(\delta) \\ \alpha M(\delta) & M(\delta) \end{bmatrix} > 0 \quad (18)$$

because

$$X_e A + A^T X_e = -Q \quad (19)$$

where

$$Q = \begin{bmatrix} 2\alpha K^* & \alpha D^* \\ \alpha D^* & 2D^* - 2\alpha M(\delta) \end{bmatrix} > 0 \quad (20)$$

from Lemmas 1 and 2.  $\square$

It is noted that stability is ensured only from the qualitative properties of sign definiteness (6) and (11) and it is independent from parameters and dimensions of the plant and controller. In the sense, the closed-loop system is robustly stable.

*Disturbance attenuation* Now we discuss conditions on feedback gain matrices  $K_{01}$  and  $K_{02}$  (11) for the closed-loop system having the prescribed disturbance attenuation ability. To this end, they are analyzed in the  $H_\infty$  optimization framework. Let us rewrite (12) in state space,

$$\dot{x} = Ax + Bw \quad (21)$$

$$z = Cx \quad (22)$$

where  $A$  is as given in (16) and

$$B = \begin{bmatrix} 0 \\ M^{-1}(\delta)L \end{bmatrix}, \quad C = [L^T \ 0] \quad (23)$$

Then, from Bounded Real Lemma (BRL), the stable transfer function  $G_{yw} = L^T(M(\delta)s^2 + D^*s + K^*)^{-1}L$  satisfies  $\|G_{yw}\|_\infty < \gamma, \forall \delta \in \mathbb{R}$  if and only if there exists a  $X > 0$  such that

$$\begin{bmatrix} XA + A^T X & XB & C^T \\ B^T X & -\gamma I & 0 \\ C & 0 & -\gamma I \end{bmatrix} < 0 \quad (24)$$

It is known that the standard  $H_\infty$  controller is feasible if the system is stabilizable and detectable (Gahinet and Apkarian [1994]). However, since our problem imposes the positive definiteness constraints (11) upon (24), it must be examined whether such a controller could exist. We can derive the following theorem.

**Theorem 2:** There always exists a controller (10) such that the closed-loop system (21)(22) has an  $H_\infty$  norm<sup>1</sup> less than  $\gamma > 0$  for all  $\delta$ .

**Proof:** From Schur complement, (24) is equivalent to

<sup>1</sup> In the strict sense of definition, we should state that the system has  $L_2$  gain less than  $\gamma > 0, \forall \delta \in \mathbb{R}$ . However, for brevity we use the term  $H_\infty$  norm throughout the paper.

$$XA + A^T X < 0 \quad (25)$$

$$XA + A^T X + \frac{1}{\gamma} [XB \ C^T] \begin{bmatrix} B^T X \\ C \end{bmatrix} < 0 \quad (26)$$

As stated in Theorem 1,  $X_e > 0$  given in (18) is a solution of (25). And from (19), (26) is

$$\frac{1}{\gamma} NN^T - Q < 0 \quad (27)$$

where  $Q > 0$  and

$$N = \begin{bmatrix} \alpha L & L \\ L & 0 \end{bmatrix}. \quad (28)$$

The inequality (27) holds for sufficiently large  $\gamma > \gamma_{min}$  for all  $\delta$ . Indeed, we can obtain the lower bound of  $\gamma$  as

$$\gamma_{min} = \lambda_{max} \left( Q^{-1/2} NN^T Q^{-1/2} \right) \quad (29)$$

by the eigen-value analysis of (27).  $\square$

*Design by LMI* In the preceding discussion, it has been shown that there exist symmetric and positive-definite feedback controller gains (11) that satisfy (24). From the design viewpoint, they are obtained by simultaneously solving (24) and (11) for all  $\delta$ . However, since (24) is a bilinear matrix inequality (BMI), there is no efficient solver. This is the general case for the static output feedback controller design. Additionally, the problem is involved because (11) and (12) must be satisfied for all  $\delta$ . To cope with the problem, we propose the following design scheme based on linear matrix inequalities (LMIs).

Let us suppose  $M(\delta)$  bounded for all  $\delta$ , and its convex decomposition given as

$$M(\delta) = \sum_{i=1}^{\sigma} a_i M_i, \quad a_i \geq 0, \quad \sum_{i=1}^{\sigma} a_i = 1 \quad (30)$$

where  $M_i$  is the mass matrix at the  $i$ th vertex formed by the maximum and minimum of entries of matrix  $M(\delta)$ . Then (27) becomes

$$\frac{1}{\gamma} NN^T - Q = \sum_{i=1}^{\sigma} a_i \left( \frac{1}{\gamma} NN^T - Q_i \right) < 0 \quad (31)$$

Therefore, if we can simultaneously solve the inequalities

$$\frac{1}{\gamma} NN^T - Q_i < 0, \quad i = 1, 2, \dots, \sigma \quad (32)$$

with (11) to obtain  $K_{01} > 0$  and  $K_{02} > 0$  so as to minimize the common  $\gamma$ , we can achieve our objective. It is noted here that  $Q_i$  in (32) is

$$Q_i = \begin{bmatrix} 2\alpha K^* & \alpha D^* \\ \alpha D^* & 2D^* - 2\alpha M_i \end{bmatrix} \quad (33)$$

from (20) and it is linear with respect to the variables  $K_{01}$  and  $K_{02}$  from (13) when the design parameter  $\alpha$  is fixed. Therefore, since (32) and (11) are LMIs, they are efficiently solved using convex optimization tools.

### 3.2 Feedforward Controller

In order to improve the attitude maneuver performance, we design feedforward controllers  $K_1$  and  $K_2$  by a model matching method. We consider to minimize  $\gamma > 0$  such that

$$\|G_r - G_{yr}\|_\infty < \gamma \quad (34)$$

for all  $\delta$ , where  $y = G_r(s)r$  denotes a given constant transfer function matrix of reference model. When the

plant is LTI, it is a standard  $H_\infty$  model matching problem to obtain  $v = [K_1^T K_2^T]^T r$ , for the generalized plant

$$z = G_r(s)r - G_{yr}v \quad (35)$$

$$y = r \quad (36)$$

However, in our LPV problem, feedforward controllers  $K_1$  and  $K_2$  must be scheduled according to the change of  $\delta$ . To this end, we consider the gain scheduling  $H_\infty$  model matching problem. Let the state equation of the feedforward controller

$$\dot{x}_k = A_k(\delta)x_k + B_k(\delta)r \quad (37)$$

$$v = C_k(\delta)x_k + D_k(\delta)r \quad (38)$$

and that of the reference model

$$\dot{x}_r = A_r x_r + B_r r \quad (39)$$

$$z_r = C_r x_r \quad (40)$$

where  $A_r$  is a constant stable matrix. The closed-loop system (12) driven by feedforward control inputs  $v_1, v_2$  are written in the following descriptor form.

$$E(\delta)\dot{x}_p = A_p x_p + B_p v \quad (41)$$

$$y = C_p x_p \quad (42)$$

where  $v = [v_1^T v_2^T]^T$  and

$$E_p(\delta) = \begin{bmatrix} I & 0 \\ 0 & M(\delta) \end{bmatrix}, \quad A_p = \begin{bmatrix} 0 & I \\ -K^* & -D^* \end{bmatrix} \quad (43)$$

$$B_p = \begin{bmatrix} 0 & 0 \\ LK_0 & L \end{bmatrix}, \quad C_p = \begin{bmatrix} L^T & 0 \\ 0 & L^T \end{bmatrix} \quad (44)$$

Then the LPV counterpart of the generalized plant used for scheduled controller design, that corresponds to LTI generalized plant (35) and (36), are from (39)(40) and (41)(42),

$$E(\delta)\dot{x} = Ax + B_1 r + B_2 v \quad (45)$$

$$z = C_1 x \quad (46)$$

$$y = r \quad (47)$$

where  $x = [x_r^T x_p^T]^T$  and

$$E(\delta) = \begin{bmatrix} I & 0 \\ 0 & E_p(\delta) \end{bmatrix}, \quad A = \begin{bmatrix} A_r & 0 \\ 0 & A_p \end{bmatrix} \quad (48)$$

$$B_1 = \begin{bmatrix} B_r \\ 0 \end{bmatrix}, \quad B_2 = \begin{bmatrix} 0 \\ B_p \end{bmatrix}, \quad C_1 = [C_r \quad -C_p] \quad (49)$$

The reason of using descriptor equation instead of state equation is twofold. First is to localize the parameter varying elements only to the mass matrix. Second is to avoid constraints encountered in solving LMIs.

The closed-loop system of the generalized plant (45)(46)(47) with the controller (37)(38) is given as

$$E_{cl}(\delta)\dot{x}_{cl} = A_{cl}(\delta)x_{cl} + B_{cl}(\delta)r \quad (50)$$

$$z = C_{cl}(\delta)x_{cl} \quad (51)$$

where  $x_{cl} = [x^T x_k^T]^T$  and

$$E_{cl} = \begin{bmatrix} E(\delta) & 0 \\ 0 & I \end{bmatrix}, \quad A_{cl} = \begin{bmatrix} A & B_2 C_k(\delta) \\ 0 & A_k(\delta) \end{bmatrix} \quad (52)$$

$$B_{cl} = \begin{bmatrix} B_1 + B_2 D_k(\delta) \\ B_k(\delta) \end{bmatrix}, \quad C_{cl} = [C_1 \quad 0] \quad (53)$$

From BRL, the optimal model matching controller (37)(38) is designed by minimizing  $\gamma > 0$  for all  $\delta$  under the condition

$$\begin{bmatrix} S + S^T & E_{cl} X C_{cl}^T & B_{cl} \\ C_{cl} X E_{cl}^T & -\gamma I & 0 \\ B_{cl}^T & 0 & -\gamma I \end{bmatrix} < 0 \quad (54)$$

where  $X > 0$  and  $S = A_{cl} X E_{cl}^T$ . The gain-scheduling controller is solved by slightly extending the standard algorithm for state equation (Apkarian et al. [1995]). First, let convex decompositions of parameter varying matrices

$$E_{cl} = \sum_{i=1}^{\sigma} a_i E_{cli}, \quad A_{cl} = \sum_{i=1}^{\sigma} a_i A_{cli} \quad (55)$$

$$B_{cl} = \sum_{i=1}^{\sigma} a_i B_{cli}, \quad C_{cl} = \sum_{i=1}^{\sigma} a_i C_{cli} \quad (56)$$

Substitution (55)(56) into (54) yields

$$\sum_{i=1}^{\sigma} a_i^2 \Phi_i + \sum_{i=1}^{\sigma} a_i a_j (\Psi_{ij} + \Psi_{ji}) < 0 \quad (57)$$

where  $j = i + 1, \dots, \sigma$ ,

$$\Phi_i = \begin{bmatrix} Y_i + Y_i^T & E_{cli} X C_{cl}^T & B_{cli} \\ C_{cli} X E_{cli}^T & -\gamma I & 0 \\ B_{cli}^T & 0 & -\gamma I \end{bmatrix} \quad (58)$$

$$\Psi_i = \begin{bmatrix} Z_{ij} + Z_{ji}^T & E_{clj} X C_{cl}^T & B_{clj} \\ C_{cli} X E_{clj}^T & -\gamma I & 0 \\ B_{cli}^T & 0 & -\gamma I \end{bmatrix} \quad (59)$$

and  $Y_i = A_{cli} X E_{cli}^T$ ,  $Z_{ij} = A_{cli} X E_{clj}$ . Therefore, if we can simultaneously solve the following inequalities at each vertex of convex decomposition

$$\Phi_i < 0, \quad \Psi_{ij} + \Psi_{ji} < 0, \quad i = 1, \dots, \sigma, \quad j = i + 1, \dots, \sigma \quad (60)$$

for vertex controllers  $A_{ki}, B_{ki}, C_{ki}, D_{ki}$  and  $X > 0$  so as to minimize  $\gamma > 0$ , the gain-scheduled feedforward controller is constructed as

$$A_k(\delta) = \sum_{i=1}^{\sigma} a_i A_{ki}, \quad B_k(\delta) = \sum_{i=1}^{\sigma} a_i B_{ki} \quad (61)$$

$$C_k(\delta) = \sum_{i=1}^{\sigma} a_i C_{ki}, \quad D_k(\delta) = \sum_{i=1}^{\sigma} a_i D_{ki} \quad (62)$$

Since inequalities (60) are reduced to LMIs by eliminating matrix variables using Parrot and Finsler's lemma (Gahinet and Apkarian [1994]), the problem is again solved using convex optimization tools.

#### 4. CONTROLLER IMPLEMENTATION

For the implementation of the proposed controller, we consider the elimination of the observation noise, and the transformation to the discrete system.

##### 4.1 Elimination of Observation Noise

It is known that the rate integrating gyro used for the attitude estimate of the ETS-VIII has some observation noises. In order to attenuate the noise, we add the following 1st order low-pass filter to the angular velocity measurement  $y_2 = \dot{\theta}$  in (3).

$$\begin{aligned} \dot{x}_f &= -\mu^2 x_f + \mu y_2 \\ y_f &= \mu x_f \end{aligned} \quad (63)$$

where  $x_f, y_f \in \mathbb{R}^3$  and  $\mu^2$  ( $\mu > 0$ )  $\in \mathbb{R}$  is the breaking point frequency of the filter. Then, the control input (10) is modified as

$$u = -K_{01}y_1 - K_{02}y_f . \quad (64)$$

By extending Theorem 1, we can show that the internal stability of the feedback closed-loop system is preserved even when the filter is added to the system. In this case, the matrix  $A$  of (16) with (63) (64) is described as

$$A = \begin{bmatrix} 0 & I & 0 \\ -M^{-1}(\delta)K^* & -M^{-1}(\delta)D & -\mu M^{-1}(\delta)LK_{02} \\ 0 & \mu L^T & -\mu^2 I \end{bmatrix} . \quad (65)$$

Then the solution  $X$  (18) is

$$X = \begin{bmatrix} K^* & \alpha M(\delta) & X_{13} \\ \alpha M(\delta) & M(\delta) & X_{23} \\ X_{13}^T & X_{23}^T & X_{33} \end{bmatrix} \quad (66)$$

$$X_{13} = -\frac{\alpha}{\mu}LK_{02}, \quad X_{23} = -\frac{1}{\mu}LK_{02}$$

$$X_{33} = \frac{1}{\mu^2}K_{02}L^T M^{-1}(\delta)LK_{02} + \frac{\alpha}{\mu^2}K_{02} .$$

Using above matrices, the Lyapunov stability condition (19) is revised as

$$XA + A^T X = -Q$$

$$Q = \begin{bmatrix} 2\alpha K^* & \alpha D^* & -\frac{1}{\mu}K^* M^{-1}(\delta)LK_{02} \\ sym & 2D^* - 2\alpha M(\delta) & -\frac{1}{\mu}D^* M^{-1}(\delta)LK_{02} \\ sym & sym & \alpha K_{02} \end{bmatrix} \quad (67)$$

where *sym* denotes the symmetric element. Then,  $X > 0$  and  $Q > 0$  are satisfied under the condition  $\alpha \gg \mu^{-1}$ . Therefore, the internal stability of the feedback closed-loop system with the filter is guaranteed by selecting the suitable  $\alpha$  for the given  $\mu$ . Here, it is noted that the  $H_\infty$  performance  $\gamma$  in the BRL might be almost same for the both of the closed-loop system with or without filter, because the maximum singular values generally have the supremum in the low frequency range. For the precise model matching in the gain scheduling, we design the feedforward controller by using the proposed method to the generalized plant including the filter (63).

#### 4.2 Transformation to Discrete System

The feedforward controller (37) (38) and the noise elimination filter (63) must be discretized for the digital on-board computer. Therefore, we transform those state equations by applying practical schemes, after they are designed as the continuous systems.

First, the filter (63) is transformed as follows by the Tustin's method for precise approximation of the discrete system.

$$x_{fd}[i+1] = A_{fd} x_{fd}[i] + B_{fd} y_2[i]$$

$$y_{fd}[i] = C_{fd} x_{fd}[i]$$

$$A_{fd} = (1 - \frac{t_s}{2}\mu^2)(1 + \frac{t_s}{2}\mu^2)^{-1}I \quad (68)$$

$$B_{fd} = C_{fd} = \sqrt{t_s}\mu(1 + \frac{t_s}{2}\mu^2)^{-1}I$$

where  $t_s$  is the sample period of the discrete system.

Next, in order to reduce the calculation load of the gain scheduling on the orbit, we apply the 1st order Euler's method to the feedforward controller (37) (38) as

$$x_{kd}[i+1] = A_{kd}(\delta) x_{kd}[i] + B_{kd}(\delta) r[i]$$

$$v[i] = C_{kd}(\delta) x_{kd}[i] + D_{kd}(\delta) r[i]$$

$$A_{kd}(\delta) = I + t_s \sum_{i=1}^{\sigma} a_i A_{ki}, \quad B_{kd}(\delta) = t_s \sum_{i=1}^{\sigma} a_i B_{ki} \quad (69)$$

$$C_{kd}(\delta) = \sum_{i=1}^{\sigma} a_i C_{ki}, \quad D_{kd}(\delta) = \sum_{i=1}^{\sigma} a_i D_{ki} .$$

By using the approximation, it is confirmed that the gain scheduling can be completed in the given sampling period 62.5 (msec).

## 5. SIMULATION RESULTS

The on-orbit attitude control experiment is planned to be performed at the end of the main mobile communication mission. The purpose is to confirm the robust stability, disturbance attenuation capability to disturbances caused by the east-west orbit control thrusters and attitude maneuver around roll and pitch axes. In order to verify the capability of the proposed controller, we perform some numerical simulations which apply the discrete control system to the continuous full order ETS-VIII model.

First, we design feedback controller gain matrices  $K_{01}$  and  $K_{02}$  so that the closed-loop system has high disturbance rejection ability. They are designed using three rigid modes and two elastic modes model ( $n = 5$ ) for four vertexes ( $\sigma = 4$ ) using LMIs (32). At design phase, the achieved minimal value is  $\gamma = 6.79$  that is disturbance attenuation ratio. On the other hand,  $\gamma = 0.024$  is calculated from (27) substituted with (70) (71) for  $\delta = 45$  (deg). The difference comes from conservativeness brought in solving LMIs. The obtained gain matrices are

$$K_{01} = \begin{bmatrix} 9.66e^{+1} & -4.31e^{-4} & 2.51e^{-2} \\ -4.31e^{-4} & 9.65e^{+1} & -6.55e^{-4} \\ 2.51e^{-2} & -6.55e^{-4} & 9.65e^{+1} \end{bmatrix} \quad (70)$$

$$K_{02} = \begin{bmatrix} 1.26e^{+3} & -1.48e^{+0} & -8.65e^{-1} \\ -1.48e^{+0} & 1.17e^{+3} & -1.14e^{+0} \\ -8.65e^{-1} & -1.14e^{+0} & 1.27e^{+3} \end{bmatrix} \quad (71)$$

For the controller, the noise elimination filter (63) is given as  $\mu^2 = 2.51$  that is decided based on the maximum elastic mode frequency and the discrete system sampling period. Then, it is confirmed that the  $H_\infty$  performance  $\gamma$  of the both closed-loop systems with and without the filter is almost the same from Fig. 4. The impulse responses of roll, pitch and yaw angles to torque disturbances caused by the east-west station keeping thrusters firing at 0 (sec) and 600 (sec) during 62.5 (msec) to positive and negative directions are shown in Fig. 5. From the cant angles of thrust vectors, the firing causes  $w = [ -0.3 \ -0.5 \ 1.8 ]$  (Nm) torque around roll, pitch and yaw. This is the major disturbance source. Additionally, in the simulations, white noises of standard deviation  $1.11e^{-4}$  (deg/sec) are added to the angular velocity measurements. The spacecraft attitudes are observed to stay between +0.002 (deg) and -0.002 (deg), which is sufficiently smaller than the given specification. On the other hand, from Fig. 6, we can



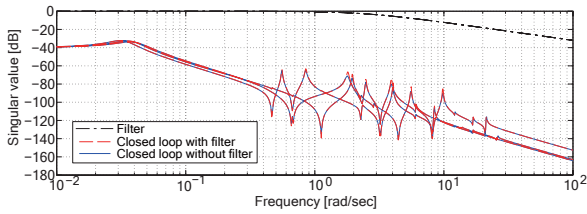


Fig. 4. Singular values of feedback closed-loop systems and noise elimination filter for paddle angle 45 [deg].

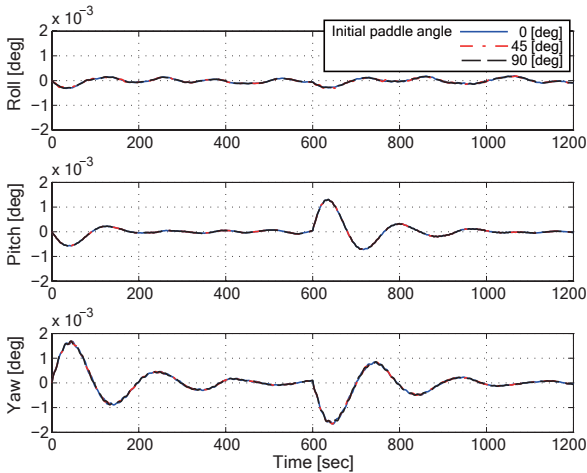


Fig. 5. Impulse responses of roll, pitch, yaw for initial paddle angles  $\delta = 0, 45, 90$  [deg].

understand that the filter is effective for reducing the noise influence to the control inputs.

Next, in order to obtain feedforward controllers  $K_1$  and  $K_2$ , we give the reference matrix  $G_r$ , so as to have

$$\frac{\omega_r^2}{s^2 + 2\zeta_r\omega_r s + \omega_r^2} \quad (72)$$

where  $\omega_r = 5.0e^{-4}$ ,  $\zeta_r = 0.7$  as its diagonal elements. By solving LMIs (60), a gain scheduling model matching controller is obtained for  $n = 5$  and  $\sigma = 4$ . In the design,  $\gamma = 0.45$  has been achieved. Simulation results of attitude maneuvering are shown in Fig. 7. They are responses to  $\pm 0.05$  (deg) step command added during 600 (sec) for each. The same white noise is also added to the angular velocity measurements in these cases. Apparently, each response well follows the reference model for all paddle angles.

## 6. CONCLUSION

This paper has proposed two-degrees-of-freedom controller as a candidate of large spacecraft ETS-VIII precise attitude control. The advantage lies in the facts that closed-loop system is ensured to be robustly stable and can be optimized using LMIs, and that high maneuver performance can be achieved. Some of simulation results were shown to demonstrate the ability.

## REFERENCES

P. Apkarian, P. Gahinet, and G. Becker. Self-scheduled  $H_\infty$  control of linear parameter-varying systems. *Automatica*, 31:1254–1261, 1995.

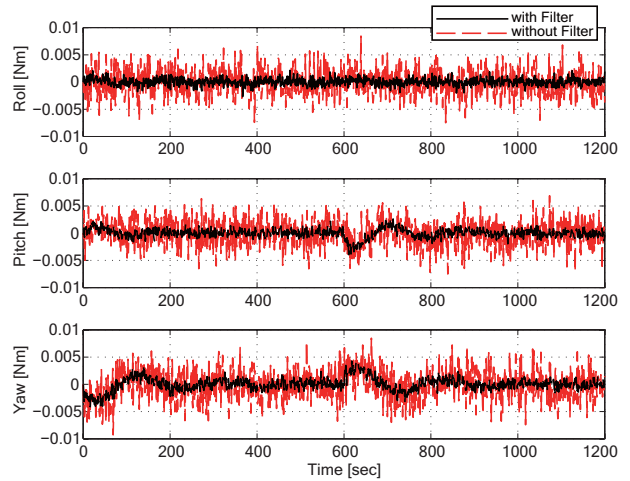


Fig. 6. Control inputs of impulse responses of roll, pitch, yaw for initial paddle angle 0 [deg].

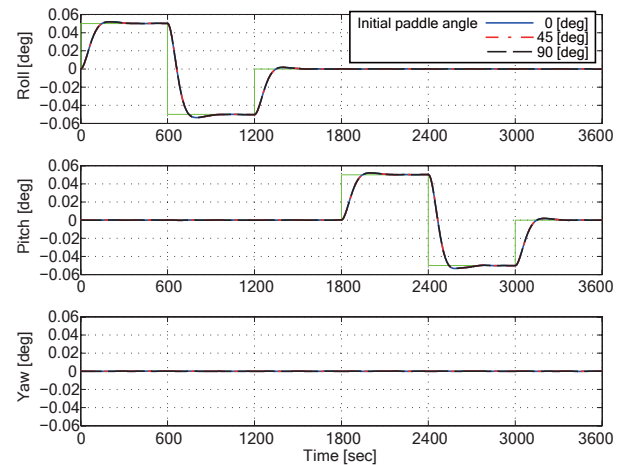


Fig. 7. Step responses of roll and yaw for initial paddle angles  $\delta = 0, 45, 90$  [deg].

P. Gahinet and P. Apkarian. A linear matrix inequality approach to  $H_\infty$  control. *Int. J. of Robust and Nonlinear Control*, 4:421–448, 1994.

Y. Hamada, T. Ohtani, T. Kida, and T. Nagashio. A new gain scheduling controller synthesis and its application to attitude control systems of a large flexible satellite. *Proc. of CDC/CACSD/ISIC 2006*, 2006.

M. Ikeda, M. Koujitani, and T. Kida. Optimality of direct velocity and displacement feedback for large space structures with collocated sensors and actuators. *12th IFAC World Congress*, VI:91–94, 1993.

S.M. Joshi. Robust properties of collocated controllers for flexible spacecraft. *J. of Guidance, Control, and Dynamics*, 9:85–91, 1986.

T. Kida, I. Yamaguchi, Y. Chida, and T. Sekiguchi. On-orbit robust control experiment of flexible spacecraft ETS-VI. *J. of Guidance, Control, and Dynamics*, 20: 865–872, 1997.

P.W. Likins. *Dynamics and control of flexible space vehicles*. JPL Technical report, 1970.

T. Nagashio and T. Kida. Three-axis attitude control of spacecraft with rotating flexible solar panels. *Proc. of IEEE International CCA*, pages 979–984, 1999.